

**Title:**

Comparative Evaluation of Pelvic Allograft Selection Methods

**Abbreviated Title**

Evaluation of Allograft Selection Methods

**Authors:**

Habib Bousleiman<sup>1</sup>

Laurent Paul<sup>2</sup>

Lutz-Peter Nolte<sup>1</sup>

Mauricio Reyes<sup>1</sup>

**Affiliations:**

1. Institute for Surgical Technology and Biomechanics, University of Bern, Stauffacherstrasse 78, CH-3014, Switzerland
2. Department of Orthopaedic Surgery, Saint-Luc University Hospital (UCL Université Catholique de Louvain), Brussels

**Corresponding Author:**

Habib Bousleiman

Phone: +41 (0) 31 631 59 48

Facsimile: +41 (0) 31 631 59 60

e-mail: habib.bousleiman@istb.unibe.ch

## **Abstract**

This paper presents a firsthand comparative evaluation of three different existing methods for selecting a suitable allograft from a bone storage bank. The three examined methods are manual selection, automatic volume-based registration, and automatic surface-based registration. Although the methods were originally published for different bones, they were adapted to be systematically applied on the same data set of hemi-pelvises. A thorough experiment was designed and applied in order to highlight the advantages and disadvantages of each method. The methods were applied on the whole pelvis and on smaller fragments, thus producing a realistic set of clinical scenarios. Clinically relevant criteria are used for the assessment such as surface distances and the quality of the junctions between the donor and the receptor. The obtained results showed that both automatic methods outperform the manual counterpart. Additional advantages of the surface-based method are in the lower computational time requirements and the greater contact surfaces where the donor meets the recipient.

## **Key terms**

Tumor resection, Orthopaedic oncology, Allograft selection, Surface registration, Volume registration, Computer-assisted surgery

## Introduction

Bone allograft reconstruction is an accepted procedure for the recovery of the original anatomy following a pathological or traumatic defect. Biological and prosthetic implants are among the various existing reconstruction methods. The choice of treatment is mostly a case-specific decision.<sup>1</sup> Despite their high complication rate and their slow incorporation into the host bed, biological massive allografts are recommended for great defects such as traumatic or pathological defects of the pelvis. Clinical reports suggest that this approach preserves the long-term bone stock and limb functionality.<sup>1,2,3,4,5,6,7</sup> Furthermore, long-term follow-up studies support and promote the use of allografts instead of prosthetic implants especially in younger patients.<sup>2,5</sup>

A poor anatomical matching between the host and the donor can alter the joint kinematics and load distribution, leading to articular fractures or joint degeneration.<sup>3,8</sup> Therefore, size and shape determination is critical to obtain an appropriate allograft.<sup>9</sup> Moreover, optimal handling of the bone bank ensures minimal loss of the usually scarce cadaver bone stock.

Access to bone allografts was facilitated with the development of centralized bone banks where bones are collected from cadavers, fresh-frozen for storage, and distributed to medical centres.<sup>10</sup> The bank systems sometime digitally store three-dimensional copies of the bones and use them for the selection process. However, the task of selecting a suitable allograft remains a major challenge.<sup>11</sup> Typically, bone banks select an appropriate donor by manually measuring anatomical dimensions on 2D radiographs.<sup>14</sup> Such a manual approach is rather subjective, time-consuming, and prone to errors. This calls for the need to introduce automated and more accurate techniques for this specific task. Figure 1a illustrates the major functions of a bone banking facility in which donors are scanned and reconstructed in 3D.<sup>9</sup>

1  
2 This work is a joint collaboration between the authors of three allograft selection methods  
3  
4 aiming to provide a comprehensive comparison and evaluation of their respective  
5  
6 performance and reliability. Although the methods were originally published for different  
7  
8 bones, they were adapted to be systematically applied on the same data set of hemi-pelvises.  
9  
10 The overall experimental design is illustrated in Figure 2. The paper starts by briefly  
11  
12 reintroducing the methods. The evaluation protocol is then described. The results and  
13  
14 statistical analysis are subsequently listed and discussed.  
15  
16  
17  
18  
19  
20  
21

22 HERE GOES FIGURE 1  
23  
24  
25

26 HERE GOES FIGURE 2  
27  
28  
29  
30

## 31 **Materials and Methods**

### 32 *Evaluated Allograft Selection Methods*

33  
34 Recent efforts aimed at developing methods capable of reliably selecting a bone fragment  
35  
36 that matches the resection-specific anatomy of the patient. Of interest to this work are three  
37  
38 conceptually different methods that share the same purpose. The first allograft selection  
39  
40 method is mostly manual but uses a computerized virtual environment.<sup>9</sup> The second bases the  
41  
42 search on image-to-image – or volume – registration.<sup>12</sup> Whereas, the third method utilizes  
43  
44 surface-to-surface registration.<sup>13</sup>  
45  
46  
47  
48  
49  
50  
51  
52

53 All three methods share the same objective, that is to find among a set of healthy bones  
54  
55 (hereafter designated as donors), the fragment(s) that closely resemble(s) the morphology of  
56  
57 the bone to be reconstructed (hereafter designated as recipient). The methods also delineate  
58  
59  
60  
61  
62  
63  
64  
65

1 the bone regions where the donor bone has to be cut to assist with the extraction of the  
2 allograft. The following paragraphs offer a brief description of the three methods under  
3 scrutiny.  
4  
5  
6  
7  
8  
9

10 *Manual Selection-* Manual selection based on 2D template comparison is the current gold  
11 standard for selecting an appropriate allograft.<sup>14</sup> A more advanced method for manual  
12 selection based on a 3D reconstruction of CT images of the available donors was proposed by  
13 Ritacco *et al.*<sup>9</sup> The computer tools and virtual environment used might vary, but the approach  
14 is unchanged. The user interacts with the virtual models and tries to adequately position and  
15 align the recipient to all donors in the bank. A subsequent visual assessment is carried out to  
16 select the most appropriate donor(s). The computer system used for this purpose consists of a  
17 dual core 2.00 GHz processor with 2GB of RAM, running under Windows<sup>®</sup> XP. In Ritacco *et*  
18 *al.*,<sup>9</sup> the authors augment the morphological information by adding three anatomical distances  
19 measured between manually placed landmark points. Figure 1c shows the landmark  
20 configuration system used in Ritacco *et al.*<sup>9</sup>  
21  
22  
23  
24  
25  
26  
27  
28  
29  
30  
31  
32  
33  
34  
35  
36  
37  
38

39 *Volume-Based Registration-* Volume-based or image-to-image registration was used in this  
40 method<sup>12</sup> to match similar objects (recipient and donor). Only rigid registration was applied in  
41 order to preserve the morphology of the bones. A similarity metric composed of intensity-  
42 based difference between voxels of two images is computed and used for the optimisation of  
43 the registration. Surface-to-surface distance was used to rank the donors and as a selection  
44 criterion. A 64-bit 8-core Intel<sup>®</sup> i7 1.60 GHz with 8 GB of RAM running under Windows<sup>®</sup> 7  
45 was used for the application of this method. Figure 3 illustrates how the rigid registration  
46 algorithm transforms one image to fit another. The authors concluded that this method is  
47 faster and more reliable than the gold standard method that they used in their previous  
48  
49  
50  
51  
52  
53  
54  
55  
56  
57  
58  
59  
60  
61  
62  
63  
64  
65

study.<sup>14</sup> In Paul *et al.*,<sup>14</sup> a two-dimensional template is printed on a transparent sheet and manually aligned with radiographs of the donors.

HERE GOES FIGURE 3

*Surface-Based Registration-* This method<sup>13</sup> is directly applied on surface representations of the bones of interest. The surfaces are composed of a dense set of points generated by segmenting CT (computed tomography) images and 3D reconstructing the individual bones (Figure 1b). An ICP-based (iterative closest point<sup>15</sup>) algorithm is applied in order to compute the transformation that results in the best fit between the recipient and a donor bone. The process is repeated until the recipient is registered to all bones in the database. Surface distance metrics are then used to select the best matching allograft(s). A 32-bit architecture, 3.00 GHz Intel® Core™ 2 Duo CPU with 3.25 GB of RAM was used for the automatic selection method. The allograft sorting and selection metric is the same used for the volume-based method. Figure 4 shows an example from the original work showing a sample result of the surface-based registration method applied on the distal femur. Surface distances are illustrated in the form of color maps for the best two and worst donors. The authors reported a significant improvement over the manual method in terms reliability and repeatability while keeping a good agreement with the gold standard. For the particular bones, the reported computation time is also considerably lower than that of the manual selection<sup>9</sup> and volume registration.<sup>12</sup> However, the study<sup>13</sup> was not meant as a comprehensive evaluation and the dataset used for the evaluation was not consistent among the different methods.

HERE GOES FIGURE 4

## Experimental Data

As mentioned in the previous section, and in order to present an unbiased evaluation and comparison, the three methods were applied on the same dataset. The dataset consists of ten left hemi-pelvises extracted from CT images of cadaveric specimens (1.0mm slice spacing, 2.7mm slice thickness, 1.0 second per 360° rotation, peak 90 kV). Each segmented hemi-pelvis was reconstructed to obtain a three-dimensional point cloud (Figure 1b). The points were triangulated to form a surface mesh of each instance for enhanced visualisation. This dataset is considered as the common ground data to be treated as donors by all three methods. An experienced surgeon applied cuts on each one of the ten hemi-pelvises in order to divide them into three separate fragments. The fragments correspond to common clinical scenarios of resection and grafting and consistent with the guidelines presented in Enneking *et al.*<sup>16</sup> The three fragments are assigned the letters A, B, and C for the iliac, acetabular, and pubic regions, respectively. The cuts are carried out using virtual planes in a 3D environment. This resulted in a total of four categories, each made of ten recipients. The first is the data set with the intact hemi-pelvis. The other three are composed of either one of the three cut out fragments. Figure 5 shows one example of the cutting configuration and the resulting junctions. A junction is defined as the contact surface between the recipient and the corresponding potential donor. In the current configuration, fragment A has one junction, whereas fragments B and C have three and two junctions, respectively. Fragments A and C are slightly less realistic as the sacroiliac and the pubic joints are not included in our analysis. However, slight relative motion is allowed at the level of these joints, a smooth and rigid transition is not as crucial as it is at the level of bone-to-bone junctions.

HERE GOES FIGURE 5

## *Testing Protocol*

The three allograft selection methods, namely manual selection, volume-based registration, and surface-based registration were applied on the datasets described earlier. An experiment is defined as the registration of every recipient to all donors in the databank and the subsequent sorting of donors in descending order of similarity to each recipient. Having four categories of recipients and one category of donors, four registration experiments were performed by each method. The first experiment considers the intact hemi-pelvis as a recipient, whereas the other three experiments use the individual fragments as recipients.

In all experiments, the databank of donors is composed of the set of intact hemi-pelvises. The measure of similarity is a method-specific quantity. The direction of the registration (definition of fixed and moving entities) also depends on the method being applied. However the results reported herein are rearranged for consistency. In total,  $10 \times 10$  (= 100) individual registrations are carried out for every experiment.

Since the recipients are extracted from the same set of donors, there will be one registration per recipient that is expected to result in a virtually perfect overlap. This hemi-pelvis will be referred to as a trap graft and was also included in the experiments. A random spatial transform (translation and rotation) was applied to all donors prior to starting the process in order to eliminate subjective biases caused by already overlapping trap grafts. The datasets were then stored under modified file names for complete experimental blindness.

Following each registration process, we used the initial cutting planes used to separate the individual fragments to extract the interfaces between the donor and recipient. For every junction, the surface area of the junctions from either side, as well as that of their intersection,



was computed. Dice coefficients<sup>17</sup> quantifying the quality of the contact surfaces at the interface between the donor and the recipient were calculated. Dice coefficients can take values within the range [0, 1], and describe the amount of overlap between two areas. Figure 6 shows an example of overlapping contact surfaces at the junction area.

We also computed surface distance metrics between the donors and the recipients. The mean surface distance consists of the average value of the individual Euclidean distances between corresponding surface points (generated using a space dividing *kd-tree*). It provides information about the overall global similarity between the two surfaces. The Hausdorff surface distance<sup>18</sup> is the largest amongst the individual Euclidean distances and it indicates the largest possible distance between the two surfaces.

HERE GOES FIGURE 6

### *Comparative Evaluation and Statistical Analysis*

In order to present a comprehensive evaluation and comparison of the methods, a set of statistical tests was designed and applied on the final outcome of the methods.<sup>19</sup> The first test is aimed to compare the ability of the different methods to correctly detect and classify the trap graft. For this purpose, Fisher's exact test was applied to check for differences between the various outcomes. The Chi-squared test was not used because some of the expected frequencies in the contingency tables were smaller than 5. A significance level of 0.05 was chosen for this and all subsequent tests.

The level of resemblance among the spectrum of results of the various methods was assessed. For every analogous pair of results, the agreement over identifying the best three donors was

determined by calculating the corresponding Cohen's kappa.<sup>20</sup> The levels of agreement are classified according to the standard interpretation of Cohen's kappa.<sup>21</sup>

In order to measure the statistical significance of the differences between different corresponding measurements, methods using analysis of variance or ANOVA were applied. Except for the processing time, the evaluation measurements were applied exclusively on the three best ranked candidate donors by each of the methods. The processing time indicates the time required by the manual or automatic selection only, without taking into account the time needed to load and unload the data from the system's memory.

## Results

In most cases, all methods were successfully able to detect the trap graft. Only for the case of fragment A (FA), the manual method failed to detect the trap graft four out of ten times. Fisher's exact test resulted in an overall  $p$ -value of 0.116, indicating a difference that is not statistically significant between the groups and therefore all three methods were able to detect the trap graft with similar performance.

HERE GOES TABLE 1

Cohen's kappa was used to assess the level of agreement of the three methods in selecting the best three candidate donors and the corresponding results are listed in Table 1. There is a general agreement between the different methods with varying levels. We did not record any cases where a clear disagreement or accidental agreement in the selection was obtained.

HERE GOES FIGURE 7

1  
2 In terms of time requirement, the manual and the volume registration methods required  
3  
4 approximately the same amount of time without evidence of significant difference. However,  
5  
6 the manual method requires continuous user input, whereas the volume-based method can be  
7  
8 ran as a background process. The surface-based method performed substantially faster. The  
9  
10 average time for a single registration required by each of the methods is compared and  
11  
12 illustrated in Figure 7. Both automatic methods have an overhead time of loading and  
13  
14 unloading the data into memory which was not included in the analysis. However, this time  
15  
16 depends on the specific hardware being used and the type of data (images or surface  
17  
18 representations).  
19  
20  
21  
22  
23  
24  
25

26  
27 HERE GOES FIGURE 8  
28  
29  
30

31  
32 Figure 8 shows a comparison of the resulting surface distances, namely, the mean and the  
33  
34 Hausdorff surface distances, between the donors and the recipients.. For all cases, the manual  
35  
36 method resulted in higher surface-to-surface distances and both automatic methods yielded  
37  
38 statistically significant improvement. However, mostly not significant differences are  
39  
40 measured between the results of the two automatic algorithms, with the exception of the  
41  
42 Hausdorff distance at fragment A.  
43  
44  
45  
46  
47

48  
49 Of high interest to the outcome of the intervention is the quality of the contact surface overlap  
50  
51 at the level of the junctions between the donor and the recipient bones. The corresponding  
52  
53 measurements are shown in Figure 9 for all junctions described in Figure 5. Interestingly, in  
54  
55 most cases the automatic methods outperform the manual counterpart, and the surface-based  
56  
57 method is often yielding the best overlap. Moreover, statistically significant differences  
58  
59  
60  
61  
62  
63  
64  
65

between the qualities of the overlap were obtained in two cases, in particular at junction 1 of fragment B and junction 1 of fragment C.

HERE GOES FIGURE 9

## Discussion

In this paper we presented a comparative evaluation of the performance of three different allograft selection methods. One manual and two automatic methods were the subject of this study. We used the pelvis as a target site due to its complex morphology, prevalence (around 30 malignant pelvis tumors per year in Argentina, 75 massive bone allografts per year in Belgium out of which 15 of the pelvis) of the procedure, and the difficulty of bone grafting in this specific location. Several criteria were used for the assessment. In particular, the ability of the methods to detect the trap grafts, the agreement between the methods over the selection and ranking of candidate donors, surface-to-surface distances between the donor and the recipient, quality of the overlap at junction levels, and required processing time. Input data was standardized for all three methods and subjective bias was eliminated.

The obtained results clearly indicated that both automatic methods outperformed the manual selection in all measured aspects while maintaining the agreement about the best three ranked donors. In contrast to the standard 2D template search,<sup>14</sup> all methods were able to accurately detect the trap graft with exceptions that are not statistically significant. This finding indicates that the manual method based on comparison of 3D models performs better than the manual method based on 2D templates,<sup>14</sup> which failed in consistently detecting the trap graft. Surface distances were largely reduced with the automatic methods. This is mostly due to the human

factor while manually aligning the donor and recipient. Moreover, there were some instances where the surface-based method resulted in statistically significant improvement over the volume-based counterpart. This result is inherent to the volume-based method that uses intensity values of images to perform the matching. The algorithm tends to be more affected by the high-intensity cortical bone than the remaining structures which might produce slight biases and misalignments. Furthermore, the image matching is done using the whole image volume where the high proportion of background voxels reduces the accuracy and increases computational time. In an actual clinical setup, the images would be cropped to cover only the volume of interest.

Moreover, our quantitative results showed a general trend where the surface-based approach results in the best quality of the overlap, whereas the manual method often comes last. The quality of surface overlap at the junctions between the donor and recipient is a major aspect that dictates the outcome of the surgery and the difficulty of the transplantation procedure. Furthermore, a smoother transition between the bones facilitates the placement of reconstruction plates and might have positive impact on the incorporation of the allograft into the host bed, thus might decrease the non-union rate. Registering a fragment to a whole pelvis will result in contact regions analogous to the junctions between the recipient and the allograft at the contact points.

Based on the obtained results, we can conclude that bone banking centres and allograft selection services could adopt the novel automatic methods. Among the direct advantages are improved quality of the selected donors and faster case processing and therefore reduced costs and higher throughput. The computational nature of the automatic methods can provide further benefits. For instance, they can be incorporated into the surgical planning pipeline to

1 guide the clinician in extracting the graft and performing the resection, and to pre-operatively  
2 visualise the possible outcomes of the surgery. One could develop a fully or partially  
3 automatic system capable of managing the problem of allograft selection with features  
4 ranging from the collection of donor bones and archiving them to accurately planning the  
5 flow of the surgery. Moreover, the application of the automatic methods is not limited to the  
6 selection of allografts. With minor adaptation, they can be used for other surgical procedures  
7 such as bone augmentation using auto- or allografts. Bone augmentation is a common  
8 technique applied in several surgical specialties such as dentistry and craniomaxillofacial.<sup>22</sup>  
9  
10  
11  
12  
13  
14  
15  
16  
17  
18  
19  
20  
21

22 Our evaluation was thorough in terms of the experimental setup and the clinical relevance of  
23 the criteria used in the analysis. However, further studies could include other anatomical  
24 regions where bone transplantation is commonly performed such as the proximal tibia or  
25 distal femur. Additionally, mechanical studies simulating the in-vivo performance of the  
26 grafts could be carried out in order to complement and further validate the design criteria  
27 presented in this and the original papers.  
28  
29  
30  
31  
32  
33  
34  
35  
36  
37  
38

### 39 **Acknowledgments**

40  
41 We would like to thank Dr. Pierre-Louis Docquier, Dr. Salman Alaraibi for carrying out the  
42 manual selection. We also thank Dr. Lucas E. Ritacco for participating in the application of  
43 the manual method and pre-processing the data. This work was carried out within the frame  
44 of the National Centre of Competence in Research, Computer-Aided and Image-Guided  
45 Medical Interventions (NCCR Co-Me), supported by the funds of the Swiss National Science  
46 Foundation (SNSF).  
47  
48  
49  
50  
51  
52  
53  
54  
55  
56  
57

### 58 **References**

59  
60  
61  
62  
63  
64  
65

1. Ozger, H., M. Bulbul, and L. Eralp. Complications of limb salvage surgery in childhood tumors and recommended solutions. *Strategies in Trauma and Limb Reconstruction* 5:11-5, 2010.
2. Matejovsky, Z., and I. Kofranek. Massive allografts in tumour surgery. *International orthopaedics* 30:478-83, 2006.
3. Muscolo, D. L., M. a Ayerza, L. Aponte-Tinao, and G. Farfalli. Allograft reconstruction after sarcoma resection in children younger than 10 years old. *Clinical orthopaedics and related research* 466:1856-62, 2008.
4. Muscolo, D. L., M. A. Ayerza, L. Aponte-Tinao, and M. Ranalletta. Partial epiphyseal preservation and intercalary allograft reconstruction in osteosarcoma of the knee. *Journal of bone and Joint Surgery* 86:2686-2693, 2004.
5. Ramseier, L. E., T. I. Malinin, H. T. Temple, W. a Mnaymneh, and G. U. Exner. Allograft reconstruction for bone sarcoma of the tibia in the growing child. *The Journal of bone and joint surgery. British volume* 88:95-9, 2006.
6. Donati, D., C. Di Bella, T. Frisoni, L. Cevolani, and H. DeGroot. Alloprosthetic composite is a suitable reconstruction after periacetabular tumor resection. *Clinical orthopaedics and related research* 469:1450-8, 2011.
7. Malhotra, R., and V. Kumar. Acetabular revision using a total acetabular allograft. *Indian journal of orthopaedics* 43:218-21, 2009.
8. Mankin, H. J., M. C. Gebhardt, L. C. Jennings, D. S. Springfield, and W. W. Tomford. Long-term results of allograft replacement in the management of bone tumors. *Clinical orthopaedics and related research* 324:86-97, 1996.
9. Ritacco, L. E., A. a Espinoza Orías, L. Aponte-Tinao, D. L. Muscolo, F. G. B. de Quirós, and I. Nozomu. Three-dimensional morphometric analysis of the distal femur: a validity

method for allograft selection using a virtual bone bank. *Studies in health technology and informatics* 160:1287-90, 2010.

10. Mankin, H., M. Gebhardt, and W. Tomford. The use of frozen cadaveric allografts in the management of patients with bone tumors of the extremities. *The Orthopedic Clinics of North America* 18:275-89, 1987.

11. Delloye, C., X. Banse, B. Birchard, P.-L. Docquier, and O. Cornu. Pelvic reconstruction with a structural pelvic allograft after resection of a malignant bone tumor. *The Journal of bone and joint surgery. American volume* 89:579-87, 2007.

12. Paul, L., P.-L. Docquier, O. Cartiaux, O. Cornu, C. Delloye, and X. Banse. Selection of massive bone allografts using shape-matching 3-dimensional registration. *Acta orthopaedica* 81:252-7, 2010.

13. Bou Sleiman, H., L. E. Ritacco, L. Aponte-Tinao, D. L. Muscolo, L.-P. Nolte, and M. Reyes. Allograft selection for transepiphyseal tumor resection around the knee using three-dimensional surface registration. *Annals of biomedical engineering* 39:1720-1727, 2011.

14. Paul, L., P.-L. Docquier, O. Cartiaux, O. Cornu, C. Delloye, and X. Banse. Inaccuracy in selection of massive bone allograft using template comparison method. *Cell and tissue banking* 9:83-90, 2008.

15. Besl, P., and N. McKay. A method for registration of 3-D shapes. *IEEE Transactions on Pattern Analysis and Machine Intelligence* 14:239-256, 1992.

16. Enneking, W. F., and W. K. Dunham. Resection and reconstruction for primary neoplasms involving the innominate bone. *Journal of bone and Joint Surgery* 60:731-746, 1978.

17. Dice, L. R. Measures of the Amount of Ecologic Association Between Species. *Ecology* 26:297-302, 1945.



- 1  
2  
3  
4  
5  
6  
7  
8  
9  
10  
11  
12  
13  
14  
15  
16  
17  
18  
19  
20  
21  
22  
23  
24  
25  
26  
27  
28  
29  
30  
31  
32  
33  
34  
35  
36  
37  
38  
39  
40  
41  
42  
43  
44  
45  
46  
47  
48  
49  
50  
51  
52  
53  
54  
55  
56  
57  
58  
59  
60  
61  
62  
63  
64  
65
18. Huttenlocher, D. P., G. a. Klanderman, and W. J. Rucklidge. Comparing images using the Hausdorff distance. *IEEE Transactions on Pattern Analysis and Machine Intelligence* 15:850-863, 1993.
19. Petrie, A. Statistics in orthopaedic papers. *The Journal of bone and joint surgery. British volume* 88:1121-36, 2006.
20. Cohen, J. A Coefficient of Agreement for Nominal Scales. *Educational and Psychological Measurement* 20:37-46, 1960.
21. Landis, J. R., and G. G. Koch. The Measurement of Observer Agreement for Categorical Data. *Biometrics* 33:159-174, 1977.
22. Greenberg, A. M., and J. Prein, eds. *Craniomaxillofacial Reconstructive and Corrective Bone Surgery*. New York, Springer, 2002.

Figure 1: (a) Bone bank system showing the different steps of freezing the bones, acquiring CT images, segmenting the volumes, and reconstructing the surfaces in 3D. (b) Surface representation of the hemi-pelvis using a dense cloud of surface points. (c) Landmark configuration for morphological measurements.

Figure 2: Overall experimental design.

1  
2  
3  
4  
5  
6  
7  
8  
9  
10  
11  
12  
13  
14  
15  
16  
17  
18  
19  
20  
21  
22  
23  
24  
25  
26  
27  
28  
29  
30  
31  
32  
33  
34  
35  
36  
37  
38  
39  
40  
41  
42  
43  
44  
45  
46  
47  
48  
49  
50  
51  
52  
53  
54  
55  
56  
57  
58  
59  
60  
61  
62  
63  
64  
65

Figure 3: Visualisation of the volume- or image-based registration result. The 2D views (A) presents the donor (orange/red) merged with the recipient (light grey). The 3D view (B) shows the general shape of both bones (white is the recipient, blue is the donor).

Figure 4: Three-dimensional view of a sample result of the surface registration method. The surface distance between the recipient and the donors from the databank is represented as color-coded surface maps. The leftmost sample is the best match, the middle one is the second best, whereas the rightmost bone is the one with the highest surface error metric. [source: Bou Sleiman *et al.*<sup>13</sup>]

Figure 5: Cutting configuration of the hemi-pelvis into three fragments. Zone I, II, and III in (FA) red, (FB) green, and (FC) blue according to the guidelines presented in Enneking *et al.*<sup>16</sup> Depending on its anatomical location and cutting planes, each fragment presents different number of donor-recipient junctions.

Figure 6: Overlap of the contact surfaces at one junction between the donor and the template.

The contours of the (white) template, (red) donor, and (green) intersection area at the junction are shown in colors.

Figure 7: Comparison of the time required for a single registration. FA, FB, and FC indicate the different fragments (\*\*\*:  $p < 0.001$ ).



Figure 8: Comparison of the post-registration (*left*) Hausdorff surface distance and (*right*) mean surface distance between the recipient and the candidate donors. FA, FB, and FC indicate the different fragments (\*:  $p < 0.05$ , \*\*:  $p < 0.01$ , \*\*\*:  $p < 0.001$ ).

Figure 9: Comparison of the dice coefficients at the junctions between the recipient and candidate donors. FA, FB, and FC indicate the difference fragments, J1, J2, and J3 indicate the different junctions (\*\*:  $p < 0.01$ ).

**Table 1:** Agreement between the different methods on the choice of the best three candidate donors using Cohen’s kappa test.  $F_A$ ,  $F_B$ , and  $F_C$  indicate the different fragments.

Agreement over best 3				
Cohen’s kappa				
Fragment	Methods	$\kappa$	CI	Agreement
Whole	Volume/Manual	0.240	0.074 – 0.576	Fair
	Surface/Manual	0.120	-0.106 – 0.346	Slight
	Surface/Volume	0.480	0.295 – 0.665	Moderate
$F_A$	Volume/Manual	0.325	0.074 – 0.576	Fair
	Surface/Manual	0.044	-0.246 – 0.333	Slight
	Surface/Volume	0.480	0.295 – 0.665	Moderate
$F_B$	Volume/Manual	0.550	0.340 – 0.761	Moderate
	Surface/Manual	0.494	0.272 – 0.716	Moderate
	Surface/Volume	0.920	0.843 – 0.997	Perfect
$F_C$	Volume/Manual	0.381	0.139 – 0.624	Fair
	Surface/Manual	0.325	0.074 – 0.576	Fair
	Surface/Volume	0.440	0.249 – 0.631	Moderate

Figure1  
[Click here to download high resolution image](#)

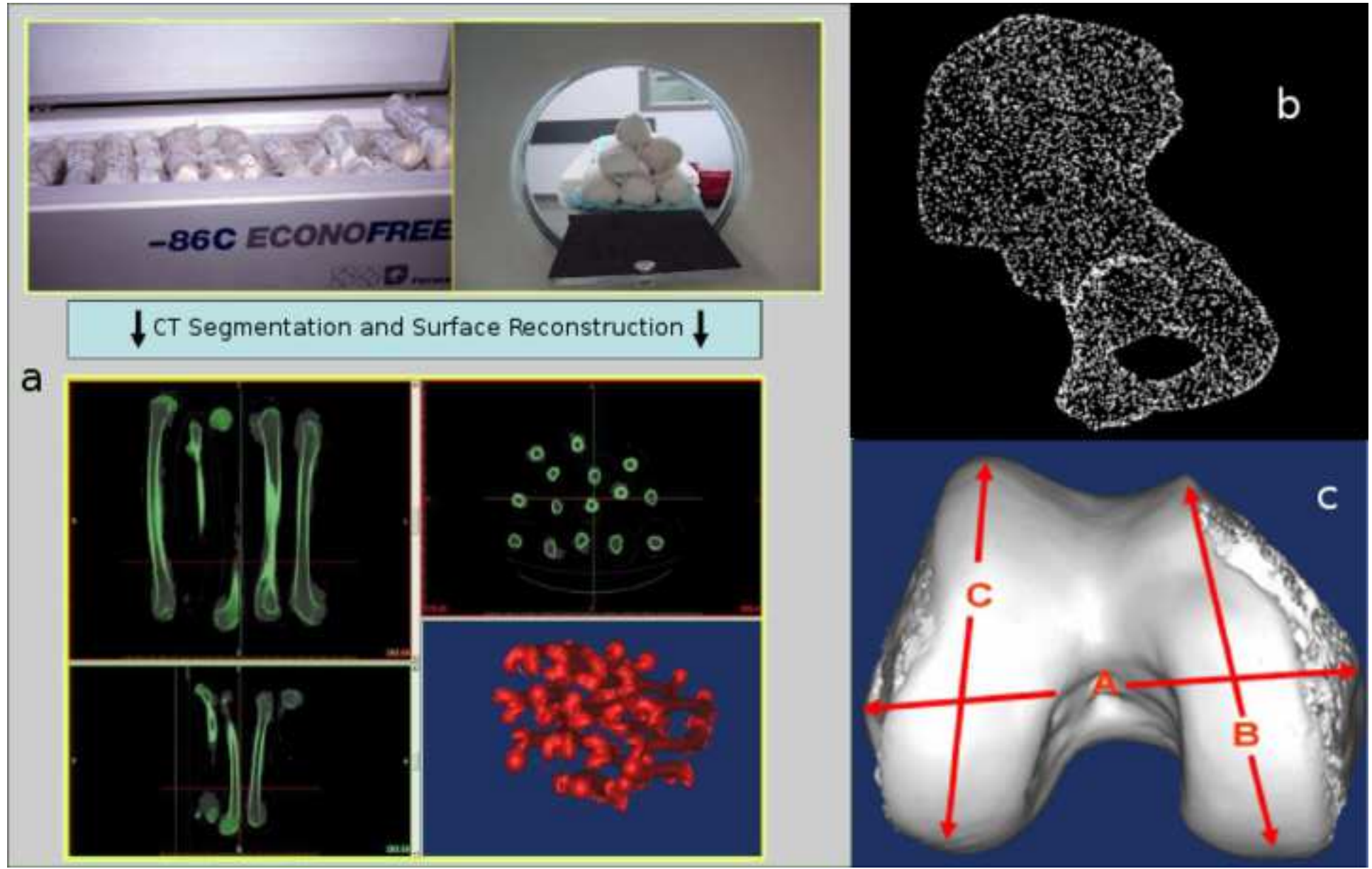


Figure2

[Click here to download high resolution image](#)

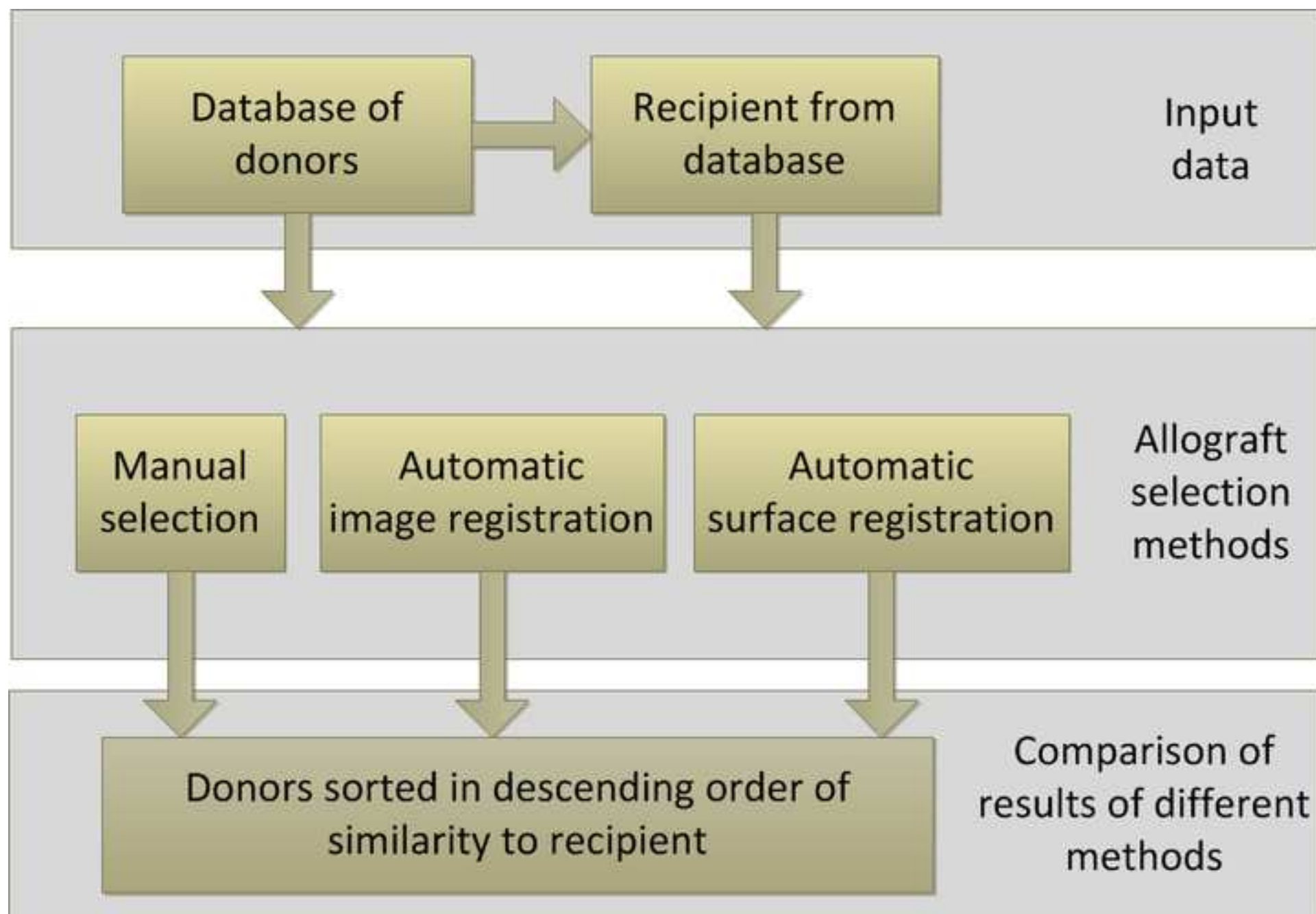


Figure3  
[Click here to download high resolution image](#)

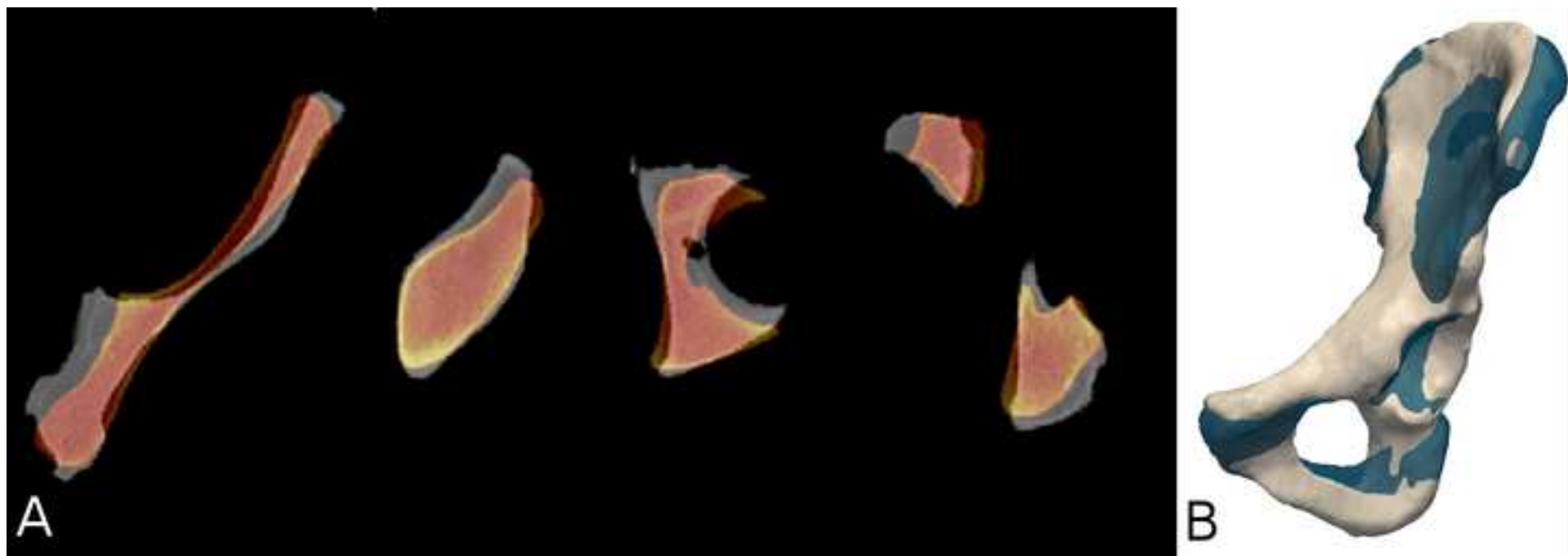


Figure4  
[Click here to download high resolution image](#)

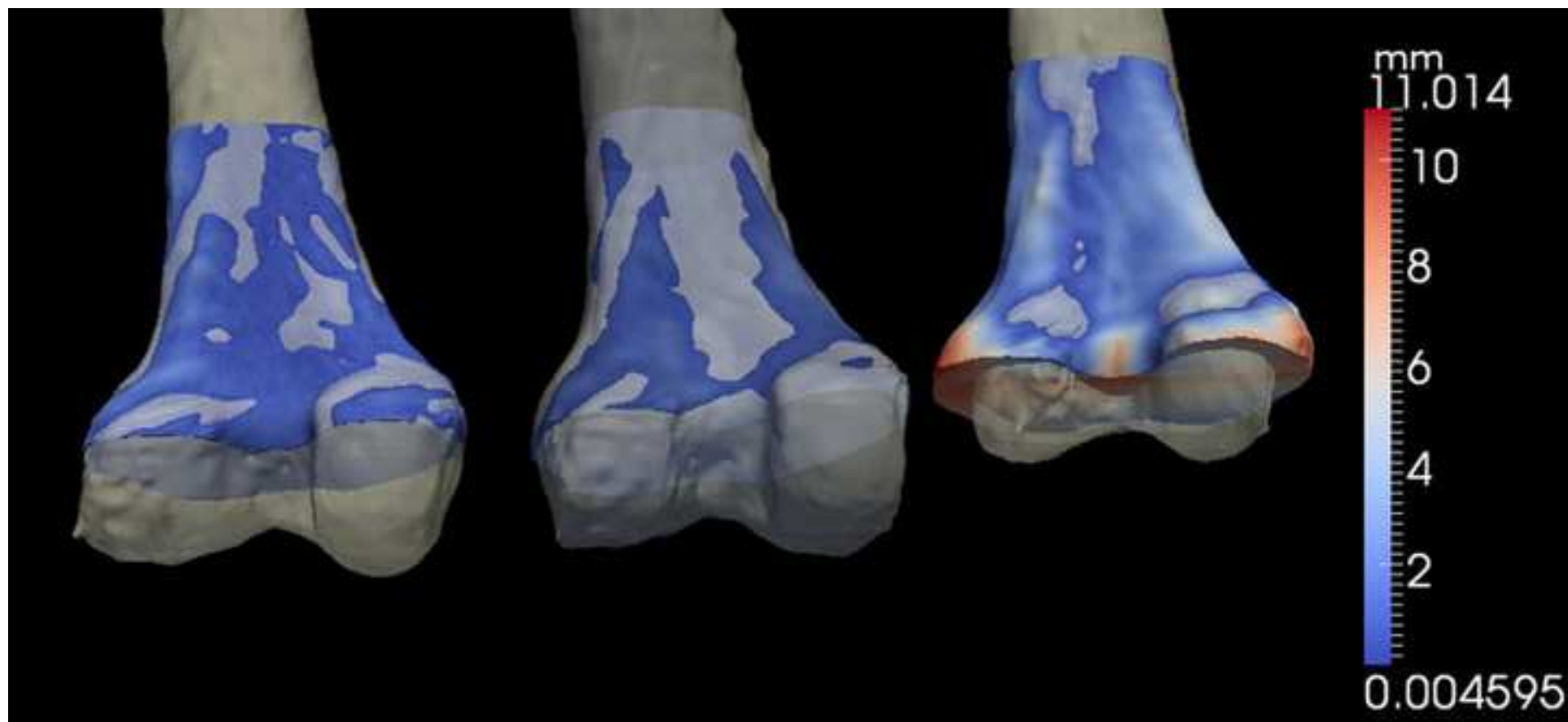


Figure5

[Click here to download high resolution image](#)

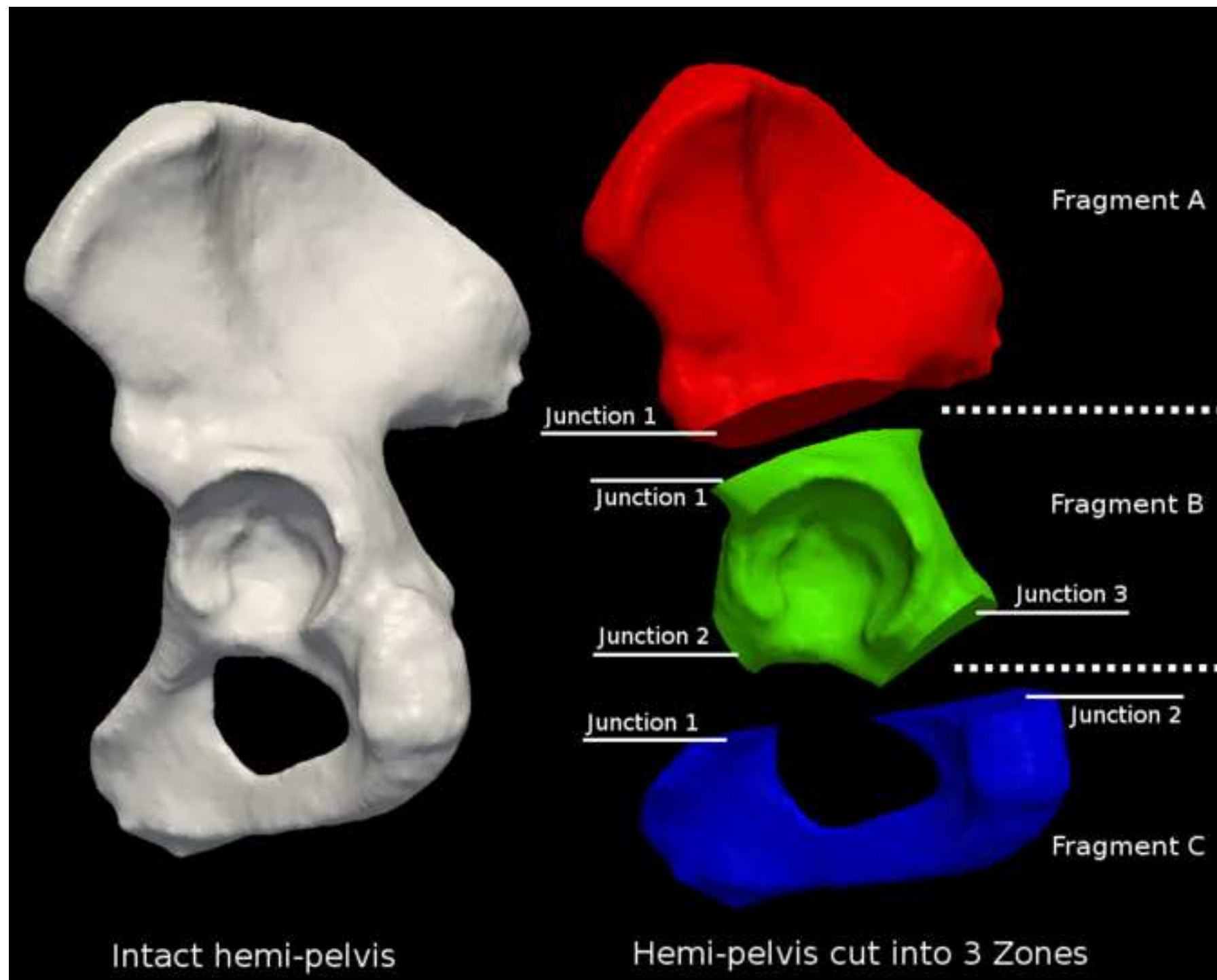




Figure6  
[Click here to download high resolution image](#)

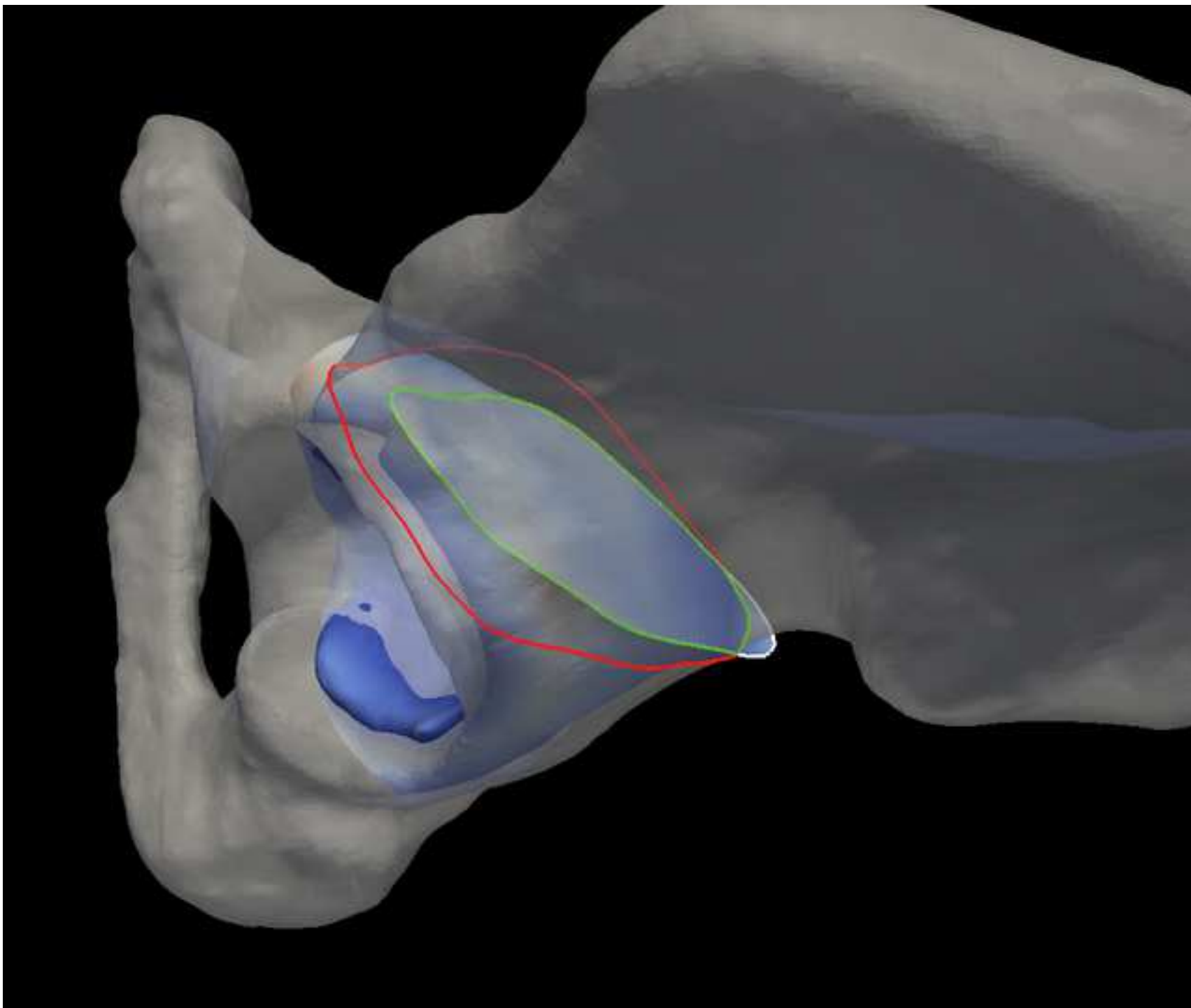


Figure7

[Click here to download high resolution image](#)

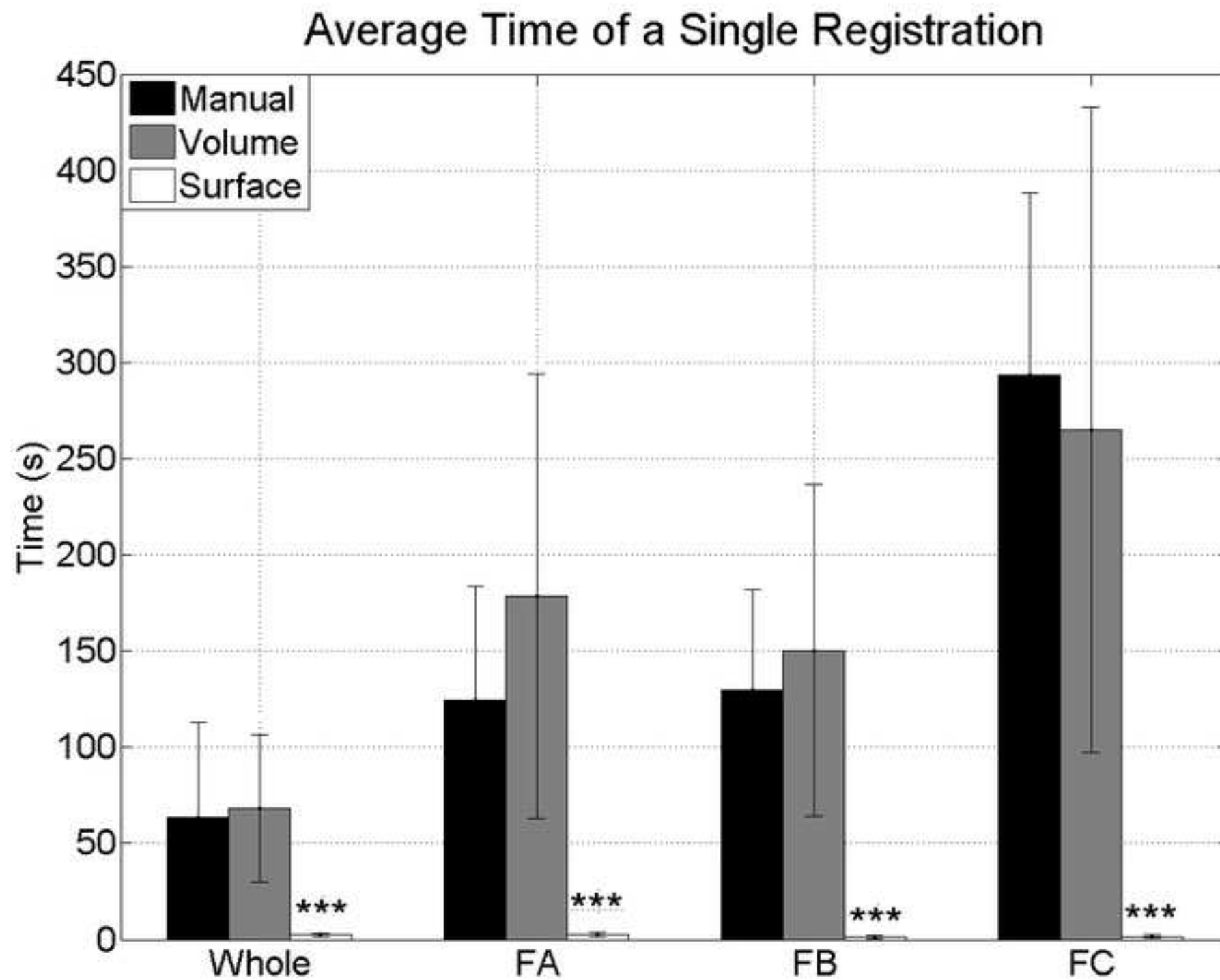


Figure8  
[Click here to download high resolution image](#)

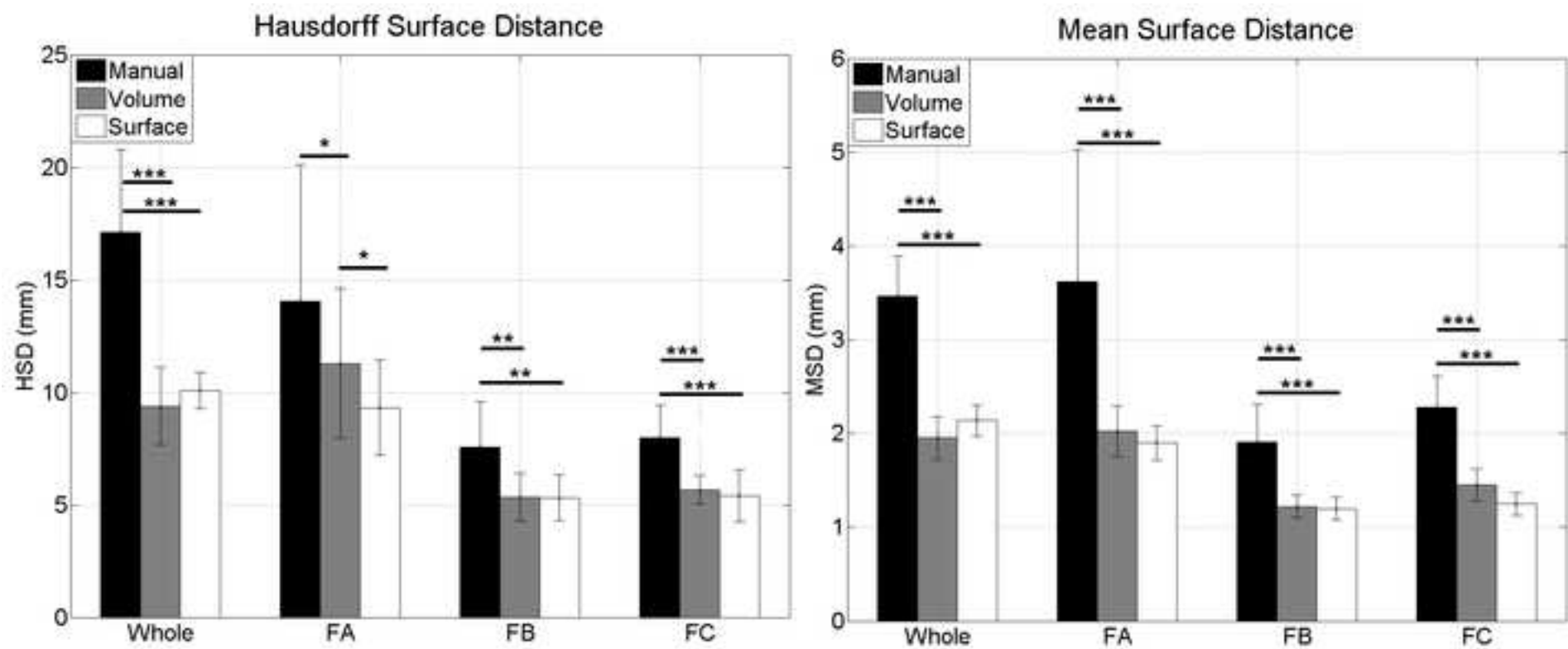
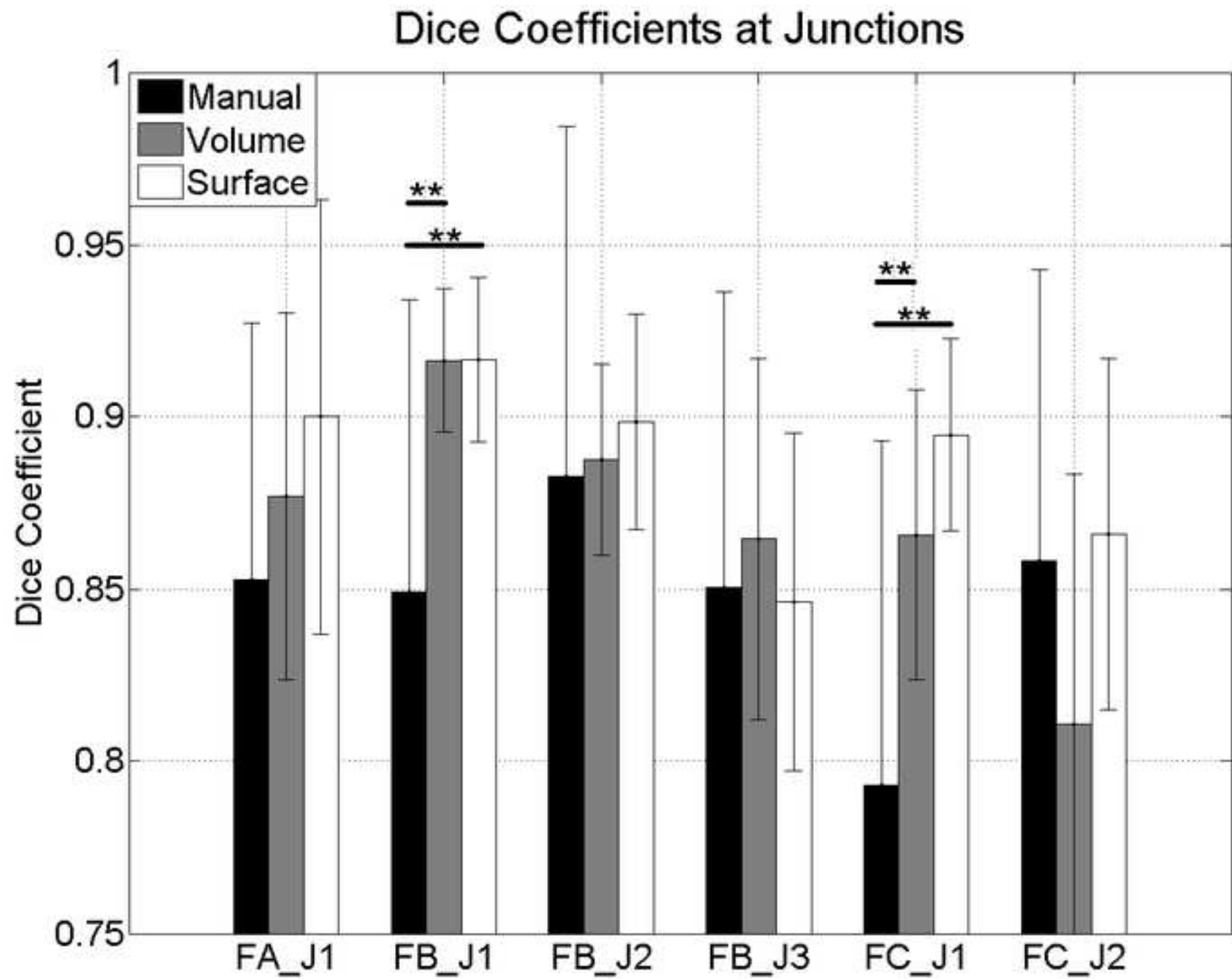


Figure9  
[Click here to download high resolution image](#)



\*Form for Disclosure of Potential Conflicts of Interest

[Click here to download Form for Disclosure of Potential Conflicts of Interest: coi\\_disclosure.pdf](#)